ELSEVIER

Journal of Photochemistry and Photobiology A: Chemistry 151 (2002) 145–155

Journal of Photochemistry and Photobiology A:Chemistry

www.elsevier.com/locate/jphotochem

A dramatic solvent effect on high-yield pulp yellowing inhibition for a benzophenone-based ultraviolet absorber

Peter McGarry [a,*], Cyril Heitner [a], John Schmidt [a], Andrew Rodenhiser [b], R. St. John Manley [b], Glen Cunkle [c], Thomas Thompson [c]

[a] *Pulp and Paper Research Institute of Canada, 570 Boul. St. Jean, Pointe-Claire, Que., Canada, H9R 3J9*
[b] *McGill University, Pulp and Paper Research Centre, 3420 University St., Montreal, Que., Canada, H3A 2A7*
[c] *Ciba Specialty Chemicals Corporation, 540 White Plains Rd., P.O. Box 2005, Tarrytown, NY, USA 10591-9005*

Received 9 April 2001; received in revised form 11 December 2001; accepted 23 January 2002

Abstract

UV screens used to photostabilise high-yield pulp do not work as well when deposited from water as they do when deposited from organic solvents. For a water-soluble ultraviolet absorber (UVA) based on 2-hydroxybenzophenone, the water-effect is dramatic. For example, during light exposure a 78% ISO brightness paper sheet made from lignin-containing peroxide bleached softwood thermomechanical pulp (BTMP) lost 27 brightness points. A BTMP sheet treated with 0.5% by weight of the UVA 5-benzoyl-4-hydroxy-2-methoxy-benzenesulfonic acid, **1** (Uvinul MS40^{TM}) delivered from ethanol lost only 19 brightness points. However, a sheet treated with 0.5% of the same UVA from water lost 25 brightness points. For a benzotriazole UVA, 5-benzotriazolyl-4-hydroxy-3-*sec*-butyl-benzenesulfonic acid, **2** (Cibafast W^{TM}) the adverse water-effect is smaller. Our experiments suggest several reasons for the poor performance of aqueous-delivered **1**: attenuation and broadening of the absorption spectra on paper when the additive is delivered from water, disruption of the internal hydrogen bond, partial formation of phenolate ion, and changes in the distribution of the additive through the thickness of the paper sheet. This effect has been found to be general across several water-soluble benzophenone- and benzotriazole-type UVAs. One exception to the rule is found for a benzotriazole that has a PEO side chain on the hydroxyphenyl ring. Thus, choice of solvent used in testing new paper stabilisers is of central importance to stabiliser performance.

Keywords: Photostabilisation; High-yield pulp; UV screen; Phosphorescence

1. Introduction

Mechanical, or high-yield pulps retain most of the lignin that is present in wood. They have high bulk, stiffness and opacity, properties that are desirable for high-quality printing and writing papers. Other benefits include efficient conversion of wood into fibre, and lower capital costs when compared with kraft pulps. A major problem limiting the wider acceptance of mechanical pulp in high-quality papers, however, is its propensity to yellow when exposed to light. Various groups have made progress in inhibiting light-induced yellowing [1–3]. McGarry et al. [4] have developed an inhibitor that gives mechanical pulp the brightness stability of bleached kraft pulp for at least 1 year. All these inhibition strategies employ ultraviolet light absorbers (UVAs) of either the 2-hydroxybenzophenone type or the 2-(2′-hydroxyphenyl)benzotriazole type, which act as efficient sunscreens to prevent damaging UV photons from reaching the lignin in the pulp.

Many research groups have reported excellent yellowing inhibition of mechanical pulp by benzotriazole and benzophenone UVAs in general [1–3,5–10], and for benzophenone UVA derivatives in particular [6,11]. Kringstad [12] first noted the ability of benzophenone UVAs to inhibit light-induced yellowing in bleached groundwood-based paper, while Castellan and coworkers [1,2] first reported the use of benzophenone UVAs in combination with reducing agents and thiols. Ragauskas and Cook [3] also reported a similar system, and showed that benzophenone UVAs are almost completely photostable on high-yield pulp. Argyropoulos et al. [14a][1] employed Allen's approach [13]

* Corresponding author. Tel.: +1-514-630-4101; fax: +1-514-630-4134.
E-mail address: pmcgarry@paprican.ca (P. McGarry).

[1] Argyropoulos attributes the drop in performance to the loss of radical scavenging ability of the tertiary amine function in the inhibitors. Since amines in general are known to darken pulps and do not inhibit yellowing [14b], we suggest that the drop in performance is due to the change in solvent for inhibitor delivery to the paper.

1010-6030/02/$ – see front matter
PII: S1010-6030(02)00029-1

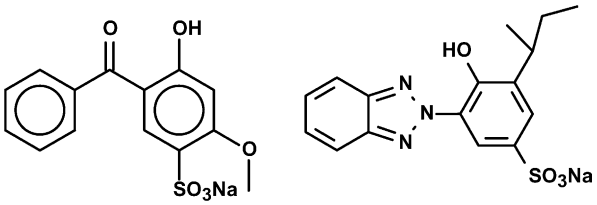

1, Uvinul MS40 **2**, Cibafast W

Fig. 1. The water-soluble benzotriazole-based UVA, Cibafast W^{TM} and the water-soluble benzophenone UVA, Uvinul MS40^{TM} are shown.

to generate hydroxybenzophenone derivatives with various Mannich bases *ortho* to the phenyl hydroxyl group, in an effort to improve compatibility with paper. In further studies, they found that intense UV irradiation of these UVAs in the presence of milled wood lignin on filter paper led to significant UVA photochemistry and degradation [15]. Thus benzotriazole and benzophenone UVAs are an important part of the search for efficient yellowing inhibitors.

Most studies of UVA inhibited light-induced yellowing in paper have involved hydrophobic UVAs which are not *water soluble*. Typically, these hydrophobic UVAs are added to the pulp from *organic solvents*. This widely accepted practice implicitly assumes that the solvent used to deliver the chemicals to the paper is immaterial to the anti-yellowing performance. Our results indicate that this assumption is *not valid*.

We report here a strong solvent effect for benzophenone and benzotriazole UVA systems (Fig. 1). We note a general decrease in activity of UVAs added to the pulp from water compared to the same UVAs added from ethanol. This adverse *water-effect* is reversed for a benzotriazole UVA with a alkaleneoxide substituent *para* to the phenolic hydroxyl group.

2. Results and discussion

Handsheets (200 g/m^2) made from lignin-containing bleached softwood thermomechanical pulp (BTMP) were treated with inhibitors according to Table 1. ISO brightness of the handsheets was recorded before and after treatment. The treated sheets were then subjected to accelerated light-induced yellowing. The post-colour (PC) number versus exposure time data is plotted in Fig. 2.

5-Benzoyl-4-hydroxy-methoxybenzenesulfonic acid (compound **1**) provided fair yellowing inhibition when applied to the handsheet from ethanol. Similar results were achieved with toluene, dioxane or methanol used as the delivery solvent. When **1** was applied from an aqueous solution, however, yellowing inhibition diminished greatly. It has been reported [16] that polyalkylene oxides improve UVA performance, but we did not observe this when polyalkalene oxides were used together with **1**. In fact, a sample treated with 1% of **1** and 0.2% PEO showed no inhibition at all. The 5 - benzotriazolyl - 4 - hydroxy - 3-*sec*-butylbenzenesulfonic acid, compound **2**, applied in an aqueous solution also exhibited an attenuated anti-yellowing ability compared to an identical sheet treated with the same additive from ethanol. Table 2 includes a list of nine different UVAs and their relative performance when introduced from water or from ethanol. The structures of these compounds are summarised in Fig. 3. A solvent effect is also evident in the study of water-soluble UVAs by Argyropoulos and coworkers [14a,b]. This study showed that the UVAs worked much better when applied from ethanol/water mixtures than from water alone. This extends the list of UVAs exhibiting a dramatic solvent effect to include eight more compounds, bringing the total to 17. Based on this data, we conclude that this is a general effect that can be considered a rule-of-thumb. The one exception to the rule is compound **4**, a benzotriazole UVA with an poly(ethylene oxide) side chain.

Overall, the UVAs investigated (except compound **4**) the detrimental water-effect averages to 6 ± 2 PC units after 13 days of accelerated photo-ageing. The reverse behaviour observed for **4** may be due to its similarity with polyoxyethylated non-ionic surfactants, such as Triton X-100, which readily form micelles [17]. In the case of micelle-like aggregation of the UVA, the intramolecular hydrogen bond (IMHB) should be stabilised in a hydrophobic region and protected from competing intermolecular hydrogen bond formation with the polar cellulose environment (The ability of **4** to form micelles is currently under investigation.).

Various experiments, discussed below, show that several factors contribute to the poor inhibition of UVAs when delivered from water.

Table 1
Accelerated photolysis of BTMP, additive loadings (percentage by weight on OD pulp) and ISO brightness

Sample	UVA (%)	Solvent	Brightness (%) (before)[a]	Brightness (%) (after)[b]	Brightness (%) (final)
1	1.0	Water/PEO	80.7	79.5	49.8
1	0.5	Organic[c]	78.1	77.8	59.2
1	0.5	Water	79.4	78.5	54.2
2	0.5	Water	77.4	78.6	60.6
2	0.5	Organic[c]	78.8	79.4	64.7
Control	–	Water	77.4	77.5	49.6

[a] Brightness before application of additive.
[b] Brightness after additive addition.
[c] Ethanol:dioxane, 1:1.

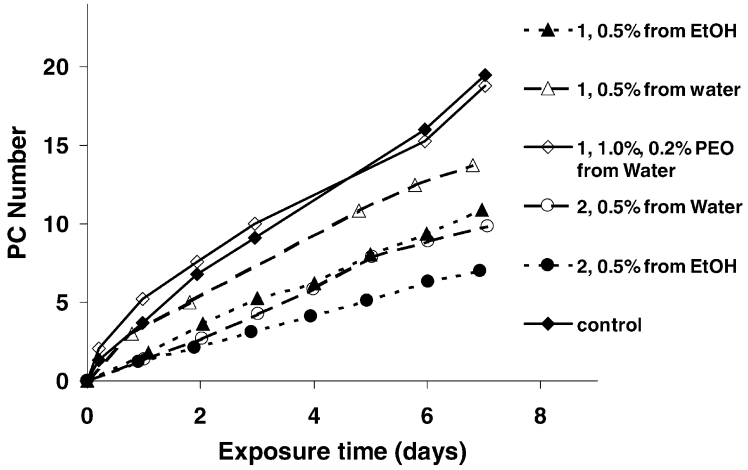

Fig. 2. A colour reversion experiment plotted as PC number versus exposure time shows that **1**, delivered to the sheet from ethanol-inhibited yellowing. The same UVA delivered from water did not inhibit yellowing very well. When 0.2% PEO was present UVA **1** provided no protection, even at twice the charge. A similar, but less dramatic, drop in activity occurred for the benzotriazole UVA, **2**. The brightness data for this experiment are listed in Table 1.

2.1. Paper chromatography

In paper chromatography experiments using water as eluent, **1** was more mobile ($R_f = 1.00$) than **2** ($R_f = 0.45$), indicating a higher polarity for **1**. This was observed both for a lignin-free kraft blotter and for a lignin-containing hardwood bleached chemithermo-mechanical pulp (BCTMP), indicating that the presence of lignin is not important. We also used ethanol as the eluent in the chromatography experiments and found that **1** ($R_f = 0.86$) was less mobile than **2** ($R_f = 1.00$) in this case, although the difference in mobility was less pronounced. The implication of the amount of movement ($R_f < 1.00$) of the two compounds is that a sidedness could result from a surface treatment of paper with the inhibitors. Thus, we evaluated the reversion inhibition of both sides of paper samples treated with UVA on one side only.

We applied the inhibitors to one side of the samples using a syringe. BTMP handsheets treated with **2** showed much better inhibition on the treated side than on the untreated side when water was used (see Fig. 4). Samples treated with **1**, however, had similar yellowing inhibition regardless of which side of the sheet was exposed. The sidedness of the two inhibitors was reversed when ethanol was used. In this case **1** had better inhibition on the treated side, whereas the sheet treated with **2** showed similar stability on both sides. One explanation consistent with these observations is that **2** performs better in water because it accumulates at the sheet surface. Surface accumulation would allow the **2** to compete more effectively for incident photons. The results in Fig. 4 infer, if yellowing inhibition is proportional to UVA concentration, that the penetration of the inhibitor through the sheet is solvent and inhibitor dependent.

The corollary to this explanation would be that water-delivered **1** fails because it is distributed into the sheet. This contradicts a mechanism proposed by Davidson et al. [16], who observed enhanced activity of UVAs in the presence of polyethylene oxide and polypropylene glycol. They asserted that the effect of the polymers was due to enhanced

Table 2
Accelerated photo-ageing of BTMP, UVAs at 0.5% by weight on OD pulp[a]

UVA	UVA type	PC number final (from water)	PC number final (from ethanol)	Solvent effect in PC number difference
1	BP	28.0	24.7	3.3
2	BZT	25.8	19.6	5.2
3	BZT	32.3	21.6	10.7
4	BZT	14.5	19.2	4.7
5	BZT	27.4	24.2	3.2
6	BZT	29.5	24.3	5.2
7	BP	29.0	25.8	3.2
8	BP	26.7	23.1	3.6
9	BP	25.0	18.9	6.1
Controls	None	30.8	29.0	1.8

[a] BP: benzophenone-type and BZT: benzotriazole-type UVAs. Structures are listed in Fig. 3. Final brightness after 13 days accelerated irradiation. All pulps samples started at between 82.7 and 82.9% ISO brightness.

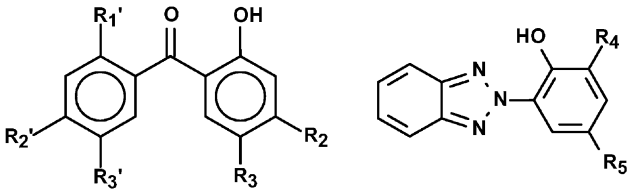

UVA	R_2	R_3	R'_1	R'_2	R'_3	R_4	R_5	R_6
3	--	--	--	--	--	*t*-Bu	$C_3H_4O_2Na$	CH_3
4	--	--	--	--	--	*t*-Bu	$C_3H_4O_2PEG$	CH_3
5	--	--	--	--	--	$C(CH_2)_2$-$PhSO_3Na$	$C(CH_2)_2$-$PhSO_3Na$	H
6	--	--	--	--	--	$CH_2N(CH_3)_2$	CH_3	H
7	OH	SO_3Na	--	--	--	--	--	--
8	OC_8H_{17}	SO_3Na	--	--	--	--	--	--
9	OCH_3	SO_3Na	OH	OCH_3	SO_3Na	--	--	--

Fig. 3. The structures of the water-soluble UVAs listed in Table 2.

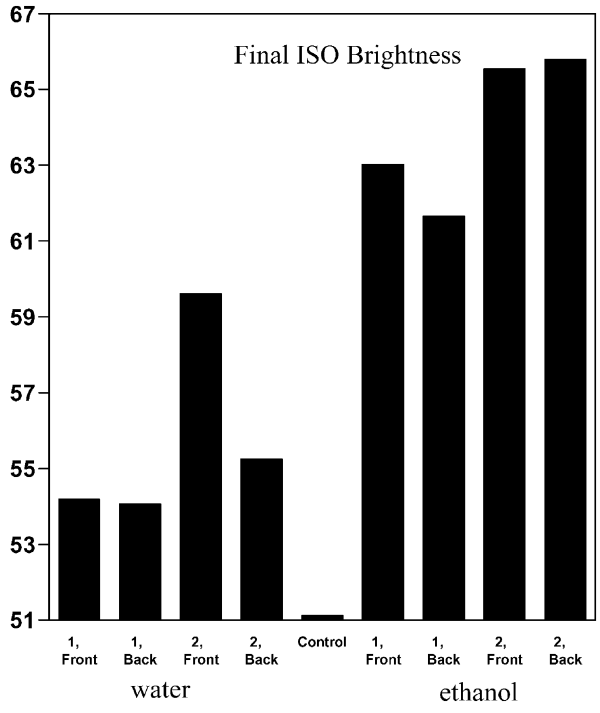

Fig. 4. The bar graph shows the final brightness of BTMP 200 g/m^2 sheets treated with 1% of **1** or **2** after 14 days of accelerated exposure. The UVAs were applied to one side via syringe. Identically treated samples were exposed on the treated side (front) and the untreated side (back). The UVA **1**, exhibited roughly the same inhibition on both sides, indicating homogeneous distribution through the thick sheet, when applied from water. Compound **2**, however, showed much better yellowing inhibition on the front side and thus likely accumulated at the surface.

distribution of the UVAs into the paper. It is also possible that the polymers could aid in localising the UVAs to the paper surface. It appears, however, that additive distribution through the thickness of the BTMP sheet is not the only factor affecting BP UVA performance.

2.2. Absorption spectra

The ethanol results point to another effect, since regardless of the sidedness the performance from ethanol was always better. Ermakova et al. [18] have shown that the acidity of phenols (both UVAs are phenolic) declined in solvents in the order: water, 50% methanol, 50% ethanol, 50% *t*-butanol, methanol, ethanol and *t*-butanol. Solution absorption spectra of **1** in water and in ethanol are shown in Fig. 5a. In water, the bands between 300 and 400 nm were slightly blue-shifted, broadened, and the absorption intensity decreased. Fig. 5b shows spectra of compound **1** as a function of pH. As pH increases, absorption between 280 and 340 nm decreases, at the same time a new peak appears between 340 and 420 nm. This new peak is attributed to the phenolate, the deprotonated form of the UVA [19]. It is apparent from comparing the spectra in Fig. 5a that some phenolate is present at neutral pH in water, while none is present in ethanol. In contrast, **2** shows only a small difference between the spectra in water and ethanol (not shown in Fig. 5 but summarised in Table 3) consistent with the known *ortho*-effect found in benzotriazoles [20].

Although solvent has an effect on the UVA solution spectra of **1**, it does not necessarily follow that the solvent used

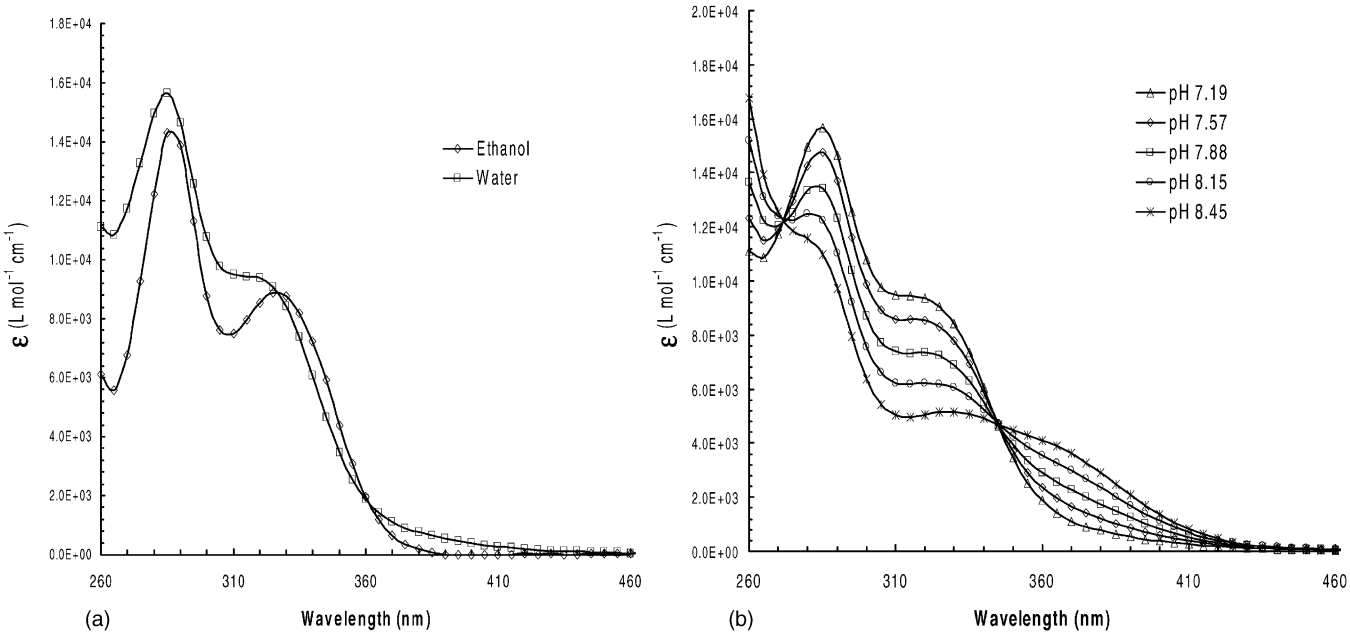

Fig. 5. (a) Solution spectra of the benzophenone UVA in alcohol and water solutions are shown for 0.10 mM solutions. In ethanol, **1** absorbed more strongly than in water. The maxima of the two wavelengths also were blue shifted in water. (b) Solution spectra of **1** as a function of pH. The equilibrium concentration of phenolate increases with pH indicated by the increasing absorption at 380 nm.

Table 3
Solvent-induced differences in solution spectra of the UVAs

UVA	Solvent	Long-wave band, λ_{max} (nm)	Short-wave band, λ_{max} (nm)
1	Ethanol	326	288
	Water	318	284
2	Ethanol	334	302
	Water	325	298

to deliver UVAs will affect their spectroscopic behaviour on the paper matrix, since the delivery solvent is removed. To examine this, we used reflectance spectroscopy to obtain absorption spectra of the UVAs adsorbed on thin sheets made from lignin-free cellulose.

The spectra of **2** on 10 g/m^2 sheets are shown in Fig. 6. We observed little difference between sheets with additive applied from water or from ethanol. It is useful to compare the peak maxima and other spectral parameters observed for the adsorbed state (Table 4) and the solution state (Table 3). In general, the absorption spectra measured on paper exhibited small shifts in the peaks to longer wavelengths. There was slight attenuation of the absorption between 300 and 380 nm, and a measurable increase in absorption between 380 and 450 nm. This latter region is where the phenolate ion absorbs [19]. The spectra of **2** on cellulose, regardless of deposition solvent, resemble the solution spectrum in ethanol.

Unlike **2**, the absorption spectra for **1** adsorbed on cellulose (Fig. 7) were affected by the deposition solvent. The absorption intensity for **1** deposited from water was up to

Table 4
Thin sheet spectroscopic parameters

UVA	Solvent	Long-wave band, λ_{max} (nm)	Short-wave band, λ_{max} (nm)
1	Ethanol	330	289
	Water	324	289
2	Ethanol	336	308
	Water	330	308

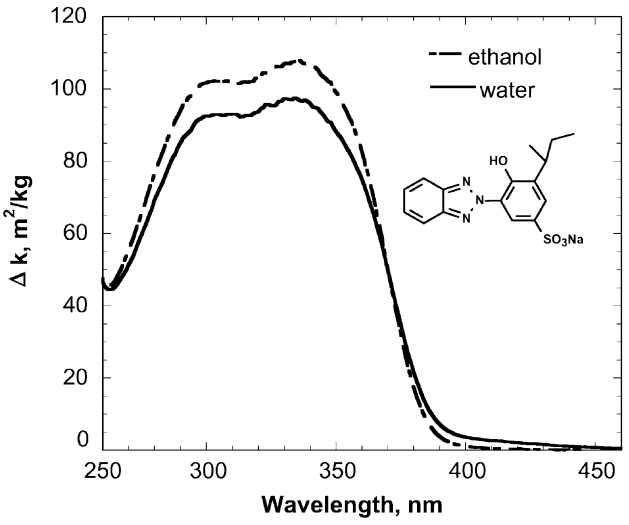

Fig. 6. Absorption spectra of **2** delivered from water and from ethanol onto lignin free cellulose fibre. The slight enhancement in absorption above 380 nm may be due to a small amount of phenolate present.

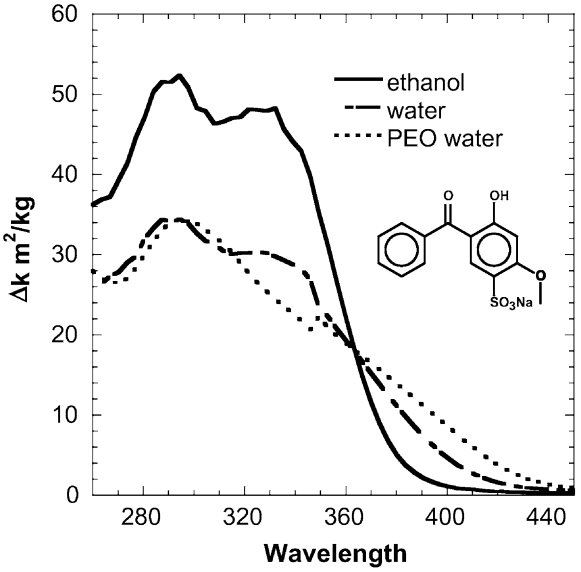

Fig. 7. Absorption spectra for **1** on lignin-free cellulose fibre are shown with the UVA delivered either from water or ethanol. The spectrum in water showed significant attenuation in intensity in the 260–350 nm region and an increase in the 380–420 nm region. This is consistent with the presence of phenolate in the sheet with the UVA delivered from water.

30% less than that for ethanol deposition, in the wavelength range between 260 and 360 nm. At wavelengths higher than 380 nm, the absorption intensity increased, an indication that phenolate ion is generated under these conditions. These effects were magnified when 0.2% of PEO was included; indeed, the discrete long-wave maximum at 330 nm disappeared completely into a long tailing absorption under these conditions.

2.3. The role of hydrogen bonding

The diminished yellowing inhibition of **1** and **2** when they are applied from water can be explained as a consequence of the two consecutive equilibria shown in Fig. 8. The first involves interconversion of the two rotamers denoted as **A** and **B** by twisting about the C–N bond joining the phenol to the benzotriazole [20–24]. Rotamer **A** is usually favoured due to the strong IMHB between the phenoxy hydrogen and the acceptor atom (nitrogen or oxygen), shown by a dashed line [24,25]. This stabilising bond is not possible for the **B** rotamer. Despite **A** being favoured, in solution it is in constant equilibrium with **B** (this is shown by the equivalence of the benzotriazole ring protons in the ^{1}H NMR spectra indicating interconversion between the **A** and **B** rotomers on the NMR timescale [21,23,26], similarly for *o*-hydroxyphenyl ketones [27,28].) In apolar environments the equilibrium lies far to the **A** side. Polar, protic environments, however, will favour the **B** form due to intermolecular H-bonding, shifting the equilibrium to the right [19,24,29,30].

The second equilibrium is the acid–base equilibrium between the phenol, **B**, and its conjugate base, the phenoxide, **C**. As the pH increases, this second equilibrium will be shifted towards **C** (we measure the pK_a of **1** and **2** to be 8.35 and 7.85, respectively). These equilibria must be operating in solution and wet paper during the addition and drying of additives. They are important to the stabilising ability of the additive because **A** is the only form that is an efficient UVA [20,22,25,31–34]. This can be understood based on the typical photochemistry of UVAs [35–42].

The unique property of UVAs is that internal conversion is so rapid that other pathways for relaxation from the excited state cannot compete [31]. All light energy absorbed is dissipated to the environment as vibrational energy (heat). This rapid internal conversion occurs when the IMHB is present, because it allows the phenoxy proton to transfer rapidly to the hydrogen bond acceptor atom (nitrogen or oxygen) and then to return. Thus **A** has an IMHB and behaves as an energy-wasting UVA. **B** and **C**, however, do not have the IMHB and will have very slow internal conversion allowing all the other possible relaxation processes to occur, including emission of light (luminescence) [25,34,36,43].

One hypothesis for the failure of UVAs when deposited to paper from water is that the concentrations of **B** and **C** are higher in water than in ethanol. Thus, more molecules are in these forms as the paper is dried from water. This is easily tested by spotting very dilute solutions of these compounds onto kraft blotter paper from either alcohol or water solution. If **1** or **2** are predominantly in form **A**, viewing them under UV light will show dark spots on the kraft blotter where the light is absorbed and energy dissipated through normal UVA action. If **B** or **C** is present, they may appear as luminescent spots on the sheet (for example, phosphorescence and fluorescence has been observed in polar solvents and matrices [24,25,40,44] and on wool fibres [45,46]). When spotted from ethanol both **1** and **2** were dark spots, thus they were predominantly in the **A** form. When these two

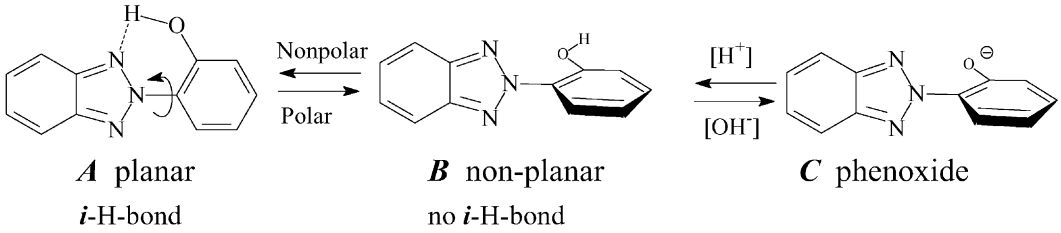

Fig. 8. Two equilibria possible for UVAs in water and alcohol are shown here. The increased polarity of water should make forms **B** and **C** more important. The planar form, **A**, is the only one expected to maintain the IMHB responsible for the UVA's ability to act as a light stabiliser.

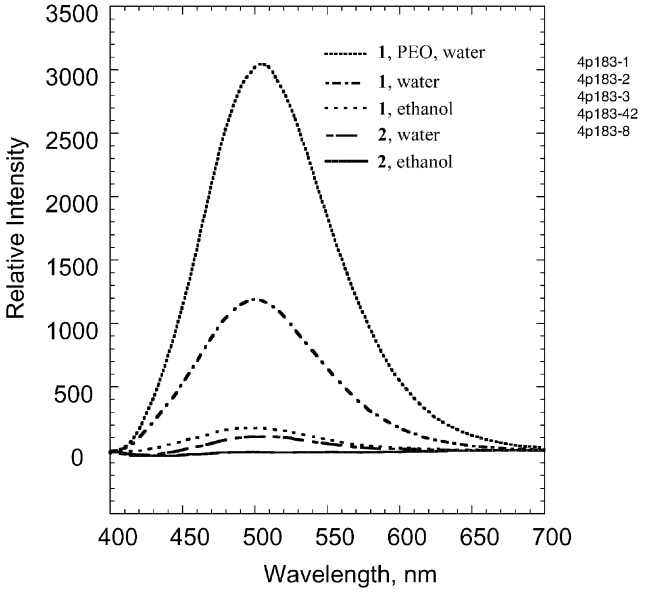

Fig. 9. Delayed emission spectra collected 40 ms after the flash. The excitation wavelength was 385 nm. Compound **1** with PEO showed the highest emission intensity, followed by **1** alone from water, **1** from ethanol, **2** from water and finally **2** from ethanol which showed no delayed emission at all.

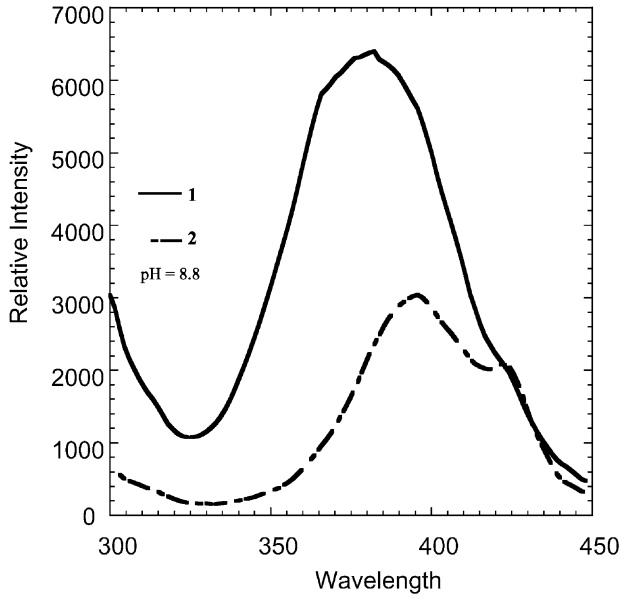

Fig. 10. Excitation spectra are shown where the exciting light was changed from 300 to 448 nm in 2 nm increments and the emission intensity was monitored at 500 nm.

additives were spotted on the paper from water, however, **1** gave a bright green luminescence, whereas the **2** remained as a dark spot. Clearly the IMHB in **1** is disrupted in water and remains disrupted upon drying the paper.

The emission was further characterised with a fluorometer with a phosphorescence attachment that is sensitive to delayed phosphorescence and excludes prompt fluorescence. As seen in Fig. 9, no phosphorescence was evident for **2** added from ethanol, and very little was measured for **2** added from water. Compound **1** exhibited a broad emission with a λ_{max} at 500 nm, typical of phosphorescence from the lowest triplet state of a benzophenone substituted at the 4 or 5 position of the phenyl ring [47]. Compound **2** also exhibited λ_{max} of 500 nm in line with that found for 2-(2′-hydroxyphenyl)benzotriazole compounds in low temperature glasses [23]. The spectra were broad and structureless, unlike those measured in low temperature glasses. This is typical of room temperature phosphorescence on paper, where the substance participates in strong hydrogen bonding with the substrate [48]. It is analogous to studies of benzophenone and benzotriazole UVAs in the photoprotection of wool fibres [45,46]. The emission intensities followed the order **2** from water < **1** from ethanol < **1** from water < **1** from water with PEO. These results match perfectly with the increased absorption observed between 350 and 450 nm in the absorption spectra for **1** and **2** (Figs. 6 and 7).

The phosphorescent species could be either **B** or **C** in Fig. 8. We further characterised the species responsible by measuring excitation spectra (Fig. 10) and kinetic decay profiles (Fig. 11). The excitation spectra indicate that the phosphorescent species has a maximum absorption at 380 nm for compound **1** and at 395 nm with a shoulder at 424 nm in the case of **2**. It is evident from the differences in these spectra that, despite the similarity in the two emission spectra shown in Fig. 9, two distinct species are responsible for the emission. The spectra shown were from samples where the UVAs were deposited from alkaline solution (pH 8.8). They are identical for samples from neutral solution except they have better signal to noise ratios. This matches nicely with assignment of the phosphorescence to the triplet of the corresponding phenolate ions. The decay profiles also corroborate this assignment to the phenolate ions of the respective UVAs. The decay of **1** is best fit with a double exponential and yields lifetimes of 0.10 and 0.85 ms (Fig. 11). It returns to baseline within 4 ms of the excitation pulse. With **2**, only a partial decay is shown in the first 4 ms. The full decay takes about 30 ms to return to baseline (inset of Fig. 11) and is best fit to a mono-exponential function which yields a lifetime of 5.4 ms or about six times the lifetime of the long-lived component of **1**. The short-lived phosphorescence for compound **1** is typical of n,π^* triplet expected for a benzophenone and the long-lived emission of **2** is typical of a π,π^* triplet consistent with a 2-(2′-hydroxyphenyl)-benotriazole chromophore. Leaver et al. [45,46] also attributed room temperature phosphorescence of UVAs on wool fibres to the respective phenolate ions.

If the delayed emission is due to the phenolate ions of **1** and **2** then phosphorescence would be enhanced further if the UVAs were introduced to the paper in their ionised forms from alkaline water. The results of an experiment where UVAs were deposited from aqueous solutions at pH

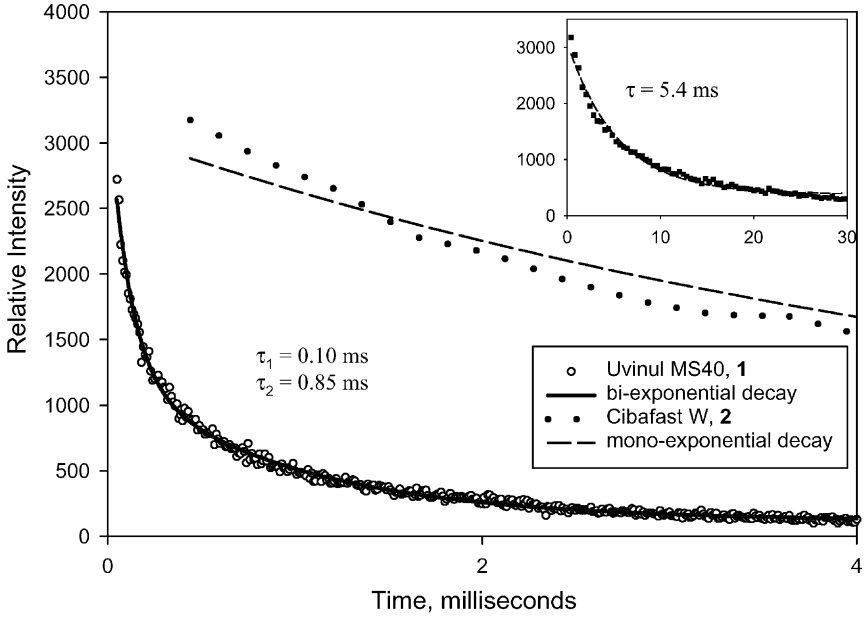

Fig. 11. Phosphorescence decays with non-linear least squares best line fits. The phosphorescence decay due to the anion of **1** is very rapid compared to that exhibited by the anion of **2**.

8.8 are shown in Fig. 12. As expected, the emission intensity increased dramatically in each case. Thus we conclude that under neutral conditions from water, substantial amounts of the phenolate of **1** are present in the paper even after drying and are responsible for a decreased anti-yellowing activity compared to addition from ethanol. In the case of **2**, however, less UVA is in the phenolate form on paper and good inhibition is maintained even when added from water.

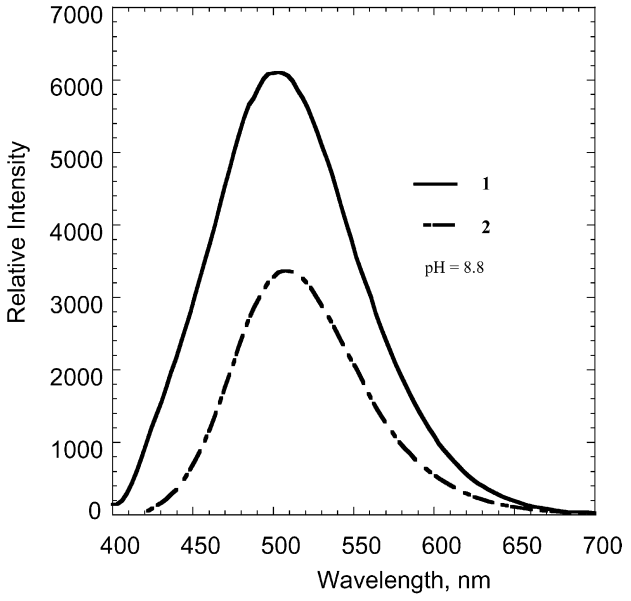

Fig. 12. Enhanced emission is obtained for both **1** and **2** when the paper is treated with additive solutions with high pH (pH = 8.8). Under these conditions **1** and **2** are in the fully ionised form (**C** of Fig. 8) when introduced to the paper. This result lends strong support to assignment of the respective phenolate ions, **C**, of **1** and **2** as the species responsible for the phosphorescence.

As an interesting aside, it is tempting to suggest that the reason UVAs in general work better at lower pH [16] is due to the effect on the two equilibria outlined earlier. The lower pH will decrease the amount of **C** [45,46] and photostabilise **B** since in its first excited state **B**'s principal mode of relaxation is to form **C** [19]. Another possibility, suggested by Davidson et al. [16], is that lignin phenolate ion concentrations are reduced. However, this should be less important since the pK_a of the UVAs (8.35 for **1** and 7.85 for **2**) are lower than that expected for most lignin phenol groups (9.4–9.9) [49].

3. Conclusion

UVAs added to paper perform more poorly when added from water than when added from ethanol or organic solvents in general. We observed this effect for nine benzophenone and benzotriazole UVAs indicating that the adverse effect of water is a general phenomenon. For an *o*-hydroxybenzophenone UVA, **1**, the decrease in performance is striking. Spectroscopic evidence indicates that the benzophenone UVA, **1**, and, to a lesser extent, the benzotriazole UVA, **2**, are partly in the phenolate form when added to cellulose fibres from water. Accelerated ageing and chromatography experiments show that distribution of the **1** through the thickness of the sheet is more homogeneous when it is added from water than when it is added from ethanol and that this adversely affects the yellowing

inhibition. Finally, substantial phosphorescence occurs for water-delivered **1**, whereas for **2** the emission intensity is weak. This luminescence indicates that a significant portion of **1** on the paper has lost the important intramolecular H-bond, and hence anti-yellowing activity. These multiple factors contribute to the dramatic drop in anti-yellowing activity of benzophenone UVAs on high-yield paper when delivered from water instead of ethanol. Thus, choice of solvent, aqueous or non-aqueous, is of crucial importance when testing chemical additives for colour stabilisation of mechanical pulp.

3.1. Experimental details

Peroxide-bleached softwood TMP (a mixture of black spruce and balsam fir) was obtained from an eastern Canadian mill. The ethanol used was the highest quality commercially available. The water-soluble UVAs employed in this study are 5-benzoyl-4-hydroxy-2-methoxy-benzenesulfonic acid, **1** (Uvinul MS40^{TM}, BASF) and 5-benzotriazolyl-4-hydroxy-3-*sec*-butyl-benzenesulfonic acid, **2** (Cibafast W^{TM}, Ciba Specialty Chemicals) were used as received. The structures of these compounds are shown in Fig. 1. Compounds **3**–**5**, **7**, and **8** were provided by Ciba Specialty Chemicals. Compound **9** was provided by BASF.

Handsheets (200 g/m^2) were prepared according to PAPTAC method C.5. The handsheets were cut into four equal (5×5 cm^2, ca. 0.50 g) squares and the ISO brightness was measured. Inhibitors were applied using a glass syringe. The amount of inhibitor required was dissolved in 1 ml of either ethanol or distilled water and applied evenly to a horizontally suspended sheet. The sheets were then placed on a contact dryer at 105 °C for 4 min and held in place by stretched felt backing.

Recently, Fernandez et al. [50] reported that a dipping method for application of inhibitors to paper is to be preferred to the drop method we used here since it provides a more homogeneous distribution of the additives studied. We prefer the drop method for the following four reasons.

1. Additives lacking fibre affinity will likely require a surface application that more resembles the drop method.
2. When water is used as the additive delivery solvent, submersion of the sheet becomes impractical since the sheet will readily disintegrate in water.
3. The distribution of the additive on the sheet will depend on its affinity for the sheet components, and hence on the chemical nature of the additives and solvent.
4. Additive distribution will be highly dependent on the method of drying the paper sheet [51]. Thus, our method also incorporates speed drying as mentioned above. This simulates industrial papermaking and promotes surface accumulation of some additives.

The inhibitor-treated brightness tabs of BTMP exhibit uniform post-treatment brightness across the square to within ±0.25% ISO at any time during the exposure testing.

Low basis weight sheets (10 g/m^2) were prepared according to a previously published procedure [52] from lignin-free kraft pulp and from the peroxide-bleached softwood TMP. Only the spectroscopic results on lignin-free paper are presented here since the short wavelength UVA bands are obscured by the lignin absorption bands on the wood-containing sheets. The low basis weight sheets were air dried. The absorption spectra changes are attenuated for high UVA charges, and when the samples are dried on a contact drier.

3.1.1. UV–Vis

Reflectance spectra were acquired with a Varian Cary 3 UV–visible spectrophotometer equipped with an external Labsphere DRA-CA-30 integrating sphere. Absorption coefficients were calculated by measuring sample reflectance over black and white backings. Complete details of the technique have been published before [53]. Absorption spectra in solution were recorded on a Hewlett-Packard 8452A diode array spectrophotometer.

3.1.2. Chromatography

An 8 in. × 8 in. kraft paper sheet (180 g/m^2) was spotted with ethanol solutions of **1** and **2**. The compounds were eluted up the sheet with distilled water. The spots were visualised using a long-wavelength UV lamp (365 nm). Compound **1** luminesced with a greenish yellow colour, whereas **2** appeared as a dark spot. Compound **1** travels with the solvent front, while **2** has an R_f of 0.45. Similar results are seen using softwood BCTMP paper.

3.1.3. Emission

Phosphorescence was measured with a SPEX Fluorolog Model-F112 spectrofluorometer equipped with a pulsed light source, a single grating excitation monochromator, a double grating emission monochromator and a 1934D phosphorescence accessory. A front-face mode with an angle of 22.5° from the excitation beam for detecting emission was employed. For emission spectra, phosphorescence was measured at every 4 nm from 400 to 700 nm with excitation centred at 385 nm. Each point represents the average of 10 lamp pulses sampled at a 0.04 ms delay for a duration of 4 ms in the case of **1** or for a duration of 10 ms for **2**. For excitation spectra, emission was monitored at a fixed wavelength of 500 nm, while the excitation wavelength was scanned from 300 to 448 nm in 2 nm intervals. Decay lifetimes for the two compounds were recorded with the excitation and the emission monochromators set to 385 and 500 nm, respectively. The emission decay profile was collected by integrating the emission intensity within a 4 or 20 ms time window as a function of an increasing delay time following the excitation lamp pulse (i.e. from 0.03 to 4 ms in 0.01 ms intervals for **1** or from 0.04 to 30 ms in 0.40 ms increments for **2**). Each point is the average of 50 lamp flashes.

3.1.4. Colour reversion experiments

For accelerated exposure, samples were placed in a LuzChem (Saint Sauveur, Que., Canada, www.luzchem.com) model XL photoreactor equipped with 24 cool white fluorescent minitube lamps according to a previously published procedure [4].

ISO brightness was recorded as a function of photolysis time with a Technidyne Micro TB-1C reflectometer according to PAPTAC method E.1, and converted to PC number as shown in Eqs. (1) and (2).

$$\mathrm{PC} = \left(\left(\frac{k}{s}\right)_{\text{after}} - \left(\frac{k}{s}\right)_{\text{before}}\right) \times 100 \quad (1)$$

$$\frac{k}{s} = \frac{(1 - R_\infty)^2}{2R_\infty} \quad (2)$$

In Eqs. (1) and (2) k and s refer to the absorption and scattering coefficients, respectively, and R_∞ is ISO brightness expressed as a fractional value. The relationship between R_∞ and the chromophore concentration is non-linear, whereas the PC number is linearly related to chromophore concentration for homogeneous samples. A smaller PC number indicates a lower chromophore concentration. While strict homogeneity of the sample is not maintained during light-induced yellowing, the PC number is still useful for qualitative comparisons.

Acknowledgements

We acknowledge the technical expertise of Jocelyn Mathieu in execution of many of the experiments reported here.

References

[1] V. Trichet, S. Grelier, A. Castellan, H. Choudry, R.S. Davidson, J. Photochem. Photobiol. A 95 (1996) 181–188.
[2] M. Petit-Conil, C. de Choudens, A. Castellan, S. Grelier, R.S. Davidson, J. Pulp Paper Sci. 24 (1998) 167.
[3] C.M. Cook, A.J. Ragauskas, J. Photochem. Photobiol. A 104 (1997) 217–224.
[4] P. McGarry, C. Heitner, J. Schmidt, R. Seltzer, G. Cunkle, J.-P. Wolf, J. Pulp Paper Sci. 26 (2000) 59–66.
[5] C. Noutary, A. Castellan, R.S. Davidson, J. Photochem. Photobiol. A 84 (1994) 317–326.
[6] P. Fornier de Violet, A. Nourmamode, N. Colombo, J. Zhu, A. Castellan, Cellulose Chem. Technol. 24 (1990) 225.
[7] M. Paulsson, A.J. Ragauskus, Nord. Pulp Paper Res. J. 13 (1998) 124–131.
[8] X. Pan, L.C. Harvey, A.J. Ragauskas, J. Pulp Paper Sci. 22 (1996) 135–140.
[9] P.A. Nolan, Paper Trade J. (Tappi Section) 121 (1945) 219.
[10] A. Castellan, C. Noutary, R.S. Davidson, J. Photochem. Photobiol. A 84 (1994) 311–316.
[11] G. Gellerstedt, I. Pattersson, S. Sundin, Svensk Papperstidning 86 (1983) R157–R163.
[12] K.P. Kringstad, Tappi J. 52 (1969) 1070.
[13] N.S. Allen, E. Haque, E.M. Howells, K. Kikkawa, M. Minigawa, Eur. Polym. J. 27 (1991) 789–794.
[14] D.S. Argyropoulos, P. Halevy, P. Peng, Photochem. Photobiol. 71 (2000) 141–148;
(b) P. Fornier de Violet, A. Nourmamode, N. Colombo, J. Zhu, A. Castellan, Cellulose Chem. Technol. 24 (1990) 225.
[15] P.P. Peng, D.S. Argyropoulos, Photochem. Photobiol. 71 (2000) 149–156.
[16] R.S. Davidson, L. Dunn, A. Castellan, A. Nourmamode, J. Photochem. Photobiol. A 86 (1995) 275–282.
[17] M.W. Samaha, V.F. Naggar, Int. J. Pharm. 42 (1988) 1–9.
[18] M.I. Ermakova, M.F. Kiryushina, M.Y. Zarubin, Khim. Drev. 6 (1985) 61–64.
[19] P.F. McGarry, S. Jockusch, Y. Fujiwara, N. Kaprinidas, N.J. Turro, J. Phys. Chem. 101 (1997) 764–767.
[20] J. Catalan, P. Perez, F. Fabero, J.F.K. Wilshire, R.M. Claramunt, J. Elguero, J. Am. Chem. Soc. 114 (1992) 964–966.
[21] J. Catalán, F. Fabero, M.S. Guijarro, R.M. Claramunt, M.D.S. Maria, M.C. Foces-Foces, F.H. Cano, J. Elguero, R. Sastre, J. Am. Chem. Soc. 112 (1990) 747–759.
[22] J. Catalán, J.C.D. Valle, F. Fabero, N.A. Garcia, Photochem. Photobiol. 61 (1995) 118.
[23] J. Reiker, E. Lemmert-Schmitt, G. Goeller, M. Roessler, G.J. Steuber, H. Schettler, H.E.A. Kramer, J.J. Stezowski, H. Hoier, S. Henkel, A. Schmidt, H. Port, M. Weichmann, J. Rody, G. Rytz, M. Slongo, J.-L. Birbaum, J. Phys. Chem. 96 (1992) 10225–10234.
[24] G. Woessner, G. Goeller, J. Rieker, H. Hoier, J.J. Stezowski, E. Daltrozzo, M. Neureiter, H.E.A. Kramer, J. Phys. Chem. 89 (1985) 3629–3636.
[25] T. Werner, J. Phys. Chem. 83 (1979) 320.
[26] A.D. Debellis, R.K. Rodebaugh, J. Suhadolnik, C. Hendricks-Guy, J. Phys. Org. Chem. 10 (1997) 107–112.
[27] S. Nagaoka, N. Hirota, M. Sumitani, K. Yoshihara, J. Am. Chem. Soc. 105 (1983) 4220–4226.
[28] S. Nagaoka, N. Hirota, M. Sumitani, K. Yoshihara, E. Lipczynska-Kochany, H. Iwamura, J. Am. Chem. Soc. 106 (1984) 6913–6916.
[29] K.P. Ghiggino, A.D. Scully, I.H. Leaver, J. Phys. Chem. 90 (1986) 5089–5093.
[30] M. Lee, J.T. Yardley, R.M. Hochstrasser, J. Phys. Chem. 91 (1987) 4621–4625.
[31] C. Chudoba, E. Riedle, M. Pfeiffer, T. Elsaesser, Chem. Phys. Lett. 263 (1996) 622–628.
[32] R. Dux, K.P. Ghiggino, O. Vogl, Aust. J. Chem. 47 (1994) 1461–1467.
[33] J. Keck, M. Roessler, C. Schroeder, G.J. Stueber, F. Waiblinger, M. Stein, D. LeGourierec, H.E.A. Kramer, H. Hoier, S. Henkel, P. Fischer, H. Port, T. Hirsch, G. Rytz, P. Hayoz, J. Phys. Chem. B 102 (1998) 6975–6985.
[34] F. Waiblinger, J. Keck, M. Stein, A.P. Fluegge, H.E.A. Kramer, D. Leppard, J. Phys. Chem. A 104 (2000) 1100–1106.
[35] G. Woessner, G. Goeller, P. Kollat, J.J. Stezowski, M. Hauser, U.K.A. Klein, E.A. Kramer, J. Phys. Chem. 88 (1984) 5544–5550.
[36] N.J. Turro, Modern Molecular Photochemistry, Benjamin/Cummings, Menlo Park, CA, 1978, pp. 375–382.
[37] G. Porter, P. Suppan, Trans. Faraday Soc. 61 (1965) 1664.
[38] S.M. Ormson, R.G. Brown, Prog. React. Kin. 19 (1994) 45–91.
[39] W. Klöpffer, Adv. Photochem. 10 (1977) 350.
[40] S.-Y. Hou, W.M. Heatherington, G.M. Korenowski, K.B. Eisenthal, Chem. Phys. Lett. 68 (1979) 282.
[41] G. Goeller, J. Reiker, A. Maier, J.J. Stezowski, E. Daltrozzo, M. Neureiter, H. Port, M. Weichmann, H.E.A. Kramer, J. Phys. Chem. 92 (1988) 1452–1458.
[42] S.J. Formosinho, L.G. Arnaut, J. Photchem. Photobiol. A 75 (1993) 21–48.
[43] F. Waiblinger, A.P. Fluegge, J. Keck, M. Stein, H.E.A. Kramer, D. Leppard, Res. Chem. Intermed. 27 (2001) 5–20.
[44] E. Orton, M.A. Morgan, G.C. Pimentel, J. Phys. Chem. 94 (1990) 7936–7943.
[45] I.H. Leaver, P.J. Waters, N.A. Evans, J. Polym. Sci. 17 (1979) 1531–1541.
[46] L.H. Leaver, J. Appl. Polym. Sci. 33 (1987) 2795–2807.

[47] O. Kysel, R. Zharadnik, Coll. Czech Chem. Commun. 35 (1970) 3030–3044.
[48] G.W. Suter, A.J. Kallir, U.P. Wild, T. Vo-Dinh, J. Phys. Chem. 90 (1986) 4941–4945.
[49] A. Platonov, A. Kurzin, E. Evstigneyev, H. Maiyorova, Proceedings of the Eighth International Symposium on Wood and Pulping Chemistry, Vol. 2, Helsinki, Finland, 1995, pp. 113–117.
[50] M.P. Fernandez, T.C. Barros, C. Bohne, J. Photochem. Photobiol. A 116 (1998) 171–177.
[51] A.C. Dreshfield, S.T. Han, Tappi 39 (1956) 449–455.
[52] J.A. Schmidt, C. Heitner, J. Wood Chem. Technol. 11 (1991) 397–418.
[53] J.A. Schmidt, C. Heitner, Tappi 76 (1993) 117–123.